Ring Laser for Precision Measurement of Nonreciprocal Phenomena

Hans R. Bilger, G. E. Stedman, M. P. Poulton, C. H. Rowe, Ziyuan Li, and P. V. Wells

Abstract—**We constructed a 0.75 m^2, square-ring laser operating at the helium–neon wavelength 633 nm (474 THz), for precision experiments in applied sciences as well as for fundamental experiments in the physics of nonreciprocal optical and other phenomena. High-quality mirrors and the absence of media, except for the He–Ne gas mixture in the beam, insure a high-quality factor of the cavity and low lock-in frequency. The Sagnac effect by the earth rotation sufficed to unlock the countercirculating modes, without the need to restore to dither, or other means of biasing, thus providing a very stable bias with a stability of the order of 1 part in 10^9. Once the ring is unlocked by this means and is in single mode excitation, the response is extremely linear in any additional frequency, whether induced mechanically or via electromagnetic fields; in the Fourier domain, all lines are equally affected by frequency pulling and by susceptibility changes. As a result, their relative positions are not affected, and their absolute frequencies may be calibrated from the earth rotational frequency. We observed a net line width of 32 ± 2 MHz. The center of the earth line is determined with a precision of about 1 mHz, that is, with a fractional precision of 1 MHz/474 THz ≈ 2×10^{-18}, which outclasses Mössbauer [1] and maser [2] lines by several orders of magnitude. This implies that it is now possible to obtain *accuracies* of such additional effects of the order of millihertz. We intend to exploit this extraordinarily high resolution in seismography, in particular shear waves, as well as in a number of physics experiments such as Fresnel drag.**

I. Introduction

In a ring laser (Fig. 1) at least two counterrotating laser beams are created in a cavity with perimeter P and area vector $\vec{A}$ (in our case $P = 3.48\ m$, and $|\vec{A}| = 0.748\ m^2$ respectively). The theory and operation have been dealt with in various publications [3]–[5]. As the beams travel in exactly the same path, any change in geometry, for example, due to temperature changes, stress of the support, and so on, affects both beams equally, and the counterrotating beam frequencies are split only by nonreciprocal phenomena. This stability has enabled the measurement of fundamental noise limits [6], [7] and has enabled us in the past to perform precision measurements of Fresnel drag [8].

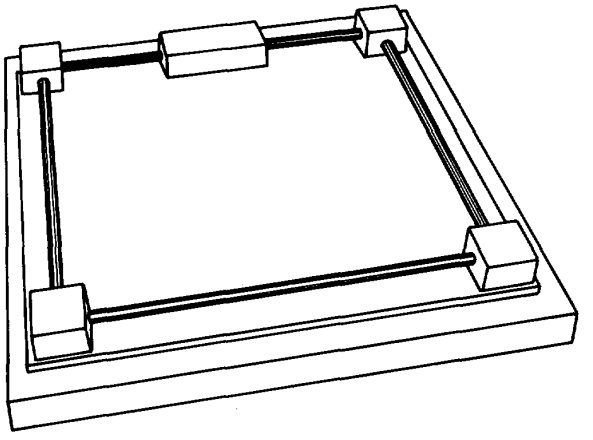

Fig. 1. Schematic of the square ring laser with four corner boxes containing highly reflective multilayer dielectric mirrors. The ring is based on a 2.54 cm thick Zerodur plate that in turn is placed on a leveled granite block of about 10 cm thickness. The upper side contains the RF excitation of the helium–neon gas. The interferometer is placed at the output of the mirror at the upper right corner. The laser beams travel inside the pyrex tubes, with no interfaces. Before filling the ring with the gas of adjustable mixing ratio and total pressure, it is evacuated to about 10^{-3} to 10^{-5} Pa.

Given a frequency-splitting phenomenon, the resulting frequency difference can easily be obtained by combining the two beams at some mirror output, where an interferometer produces a running fringe pattern such that a corotating detector observes precisely the beat frequency.

Ring lasers thus act as differential sensors for effects that influence the two counterrotating beams differently. No external reference is in principle needed, and frequency differences in the microhertz range can be established with suitable measuring time lengths. As this is done with optical frequencies of the order of 10^{15} Hz, the achievable sensitivities for such phenomena as Faraday effect, Fresnel drag, magnetic-field induced changes of the index or refraction [9], mechanical rotation, and so on are correspondingly high.

II. Construction of Ring Laser and First Results

The ring laser has a nearly square, plane geometry. The ring geometry is defined by highly reflecting multilayer dielectric mirrors with original reflectance of 99.9985%

Manuscript received June 12, 1992; revised October 13, 1992. H. R. Bilger was supported in part by the NSF. This work was also supported by the US-NZ Cooperative Science Program, two Erskine Fellowships given by Canterbury University, and the Prince of Wales Foundation.

H. R. Bilger is with the School of Electrical and Computer Engineering, Oklahoma State University, Stillwater, OK 74078-0321.

G. E. Stedman, M. P. Poulton, C. H. Rowe, Z. Li, and P. V. Wells, are with the Department of Physics and Astronomy, University of Canterbury, Christchurch 1, New Zealand.

IEEE Log Number 9206480.

for s-reflection as measured in a ring-down cavity. Ultra-high vacuum coated SiO_2-TiO_2 $\lambda/4$ layers give losses of 4 ppm due to scattering (TIS), 4 ppm from transmission and absorption (by difference) of 7 ppm, approaching that of the bulk materials. For further mechanical and thermal stability the mirrors are mounted in superinvar holders resting on a 1×1 m^2 Zerodur plate, itself on a granite base. The stainless steel corner boxes avoid mechanical contact with the mirrors; their bottoms are open and are sealed by Viton O-rings against the Zerodur plate. The corners are connected with each other by pyrex tubes (see Fig. 1) which also contain the helium–neon mixture. The beams can easily be accessed with electric and magnetic fields. To insert material media into the beams, Brewster or antireflection windows have to be introduced.

High-frequency (RF) excitation for the HeNe plasma amplifier is chosen at various frequencies between 10 and 50 MHz. This mode of excitation has the advantage of easy adjustability; it avoids biasing effects like Langmuir flow [5], and it obviates the need for internal electrodes. The ring presents no interfaces to the beam; that is, the beam travels through the HeNe mixture only. The mixture ratio and the total pressure are variable. The present results below are obtained with a natural isotope mixture, although we intend to use an isotope mix $Ne^{20}:Ne^{22} = 54:46$ [5] in the future, for better control on the composite gain curve.

All data were taken while the ring operated in single longitudinal gaussian mode, as observed on a high-resolution Fabry–Perot with a free spectral range of 6 GHz and an observed finesse $\simeq$ 60000 (NL-1 from Newport). Starving out all but one mode proved to be surprisingly easy, despite the relatively small longitudinal mode spacing of 86 MHz. Our applications require small bandwidths—typically less than 1 Hz—and therefore need only low beam power for an adequate signal/noise ratio. We had previously estimated that reducing the gain to the point when the output beam power was approximately 30 nW would suffice to starve out all but one mode; the measured output beam power under single mode operation was typically 16 nW.

The ring-down decay time is $\tau = 15\ \mu s$, which translates into a quality factor $Q = \omega\tau = 4.5 \times 10^{10}$. This value is substantially lower than that given through the reflectivity of the mirrors above because of contamination.

After several (up to eight) hours of operation, the locking frequency increases noticeably, and ultimately the ring locks. This is due to contamination of the gas; the prototype uses Viton O-rings for ease of assembly. Fortunately, the ring may be regenerated essentially to its previous level of performance by thorough pump-down and a gas refill. It seems that this contamination is associated with the O-rings. It affects the gas much more than the mirrors. A next generation ring now under design avoids O-rings altogether. Independently of this, we also observed slowly increasing mirror damage, which could only partially be restored by special cleaning and annealing by the manufacturer. This appears to be related to our initial use of an oil-diffusion pump, albeit with a liquid nitrogen cold trap; a turbomolecular pump and mass spectrometric leak detector system are presently being installed.

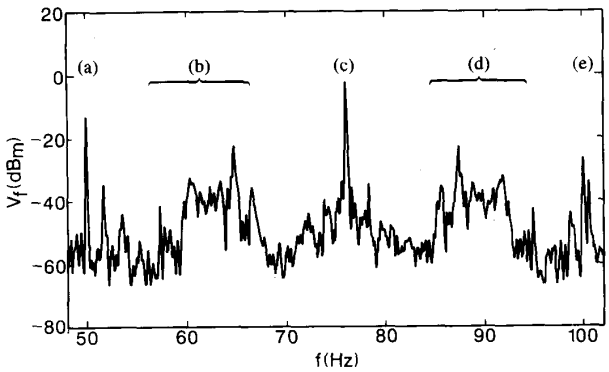

Fig. 2. Spectral analysis of the ring laser output in the frequency range 48 Hz–102 Hz. Identification of lines: a) 50 Hz for vibration due to fundamental power line frequency, b) lower sideband with prominent peaks at 11.306 Hz below and above the earth line. This is due to torsional oscillations of the ring laser base, c) earth line, d) upper sideband, symmetric to lower sideband b, due to the same causes, e) 100 Hz harmonic of power line frequency. Not shown are the harmonics of the earth line at 152 Hz and 228 Hz (analyzed in [16]), larger satellite frequencies of the 50 Hz sideband, and the fundamental frequencies of the rotation of the ring laser base in the frequency range 9–25 Hz.

For an initial demonstration of the operation of our ring we observed the frequency splitting due to the earth rotation. The beat frequency between the counterrotating beams of a ring operating at wavelength λ, that is subjected to a rotation $\vec{\Omega}$, is given by the Sagnac equation

$$\Delta f = 4\vec{\Omega} \cdot \vec{A}/(\lambda P). \tag{1}$$

The ring is placed level. At Christchurch (latitude 43° 29′), where the ring is working, we expect a beat frequency of 68.5 Hz. Fig. 2 shows one of the spectra obtained from ring output for a duration of $T = 16.384$ s, with a sampling rate of 500 s^{-1}. It may be emphasized again that no extra frequency splitting was introduced; the ring is free-running, subject only to the earth rotation. The ring laser output was prefiltered with a simple low-pass filter of bandwidth 500 Hz.

We observe several characteristic features. The peak at 76 Hz is due to the earth rotation (the next two harmonics have been observed as well). The noise power spectral density is approximately 32 dB below the observed peak and constant in the observed frequency range of 0.2–250 Hz. The peaks at 50 Hz and at 100 Hz are most probably due to residual power line hum, that is, modulation of the RF-excitation power by the electricity mains supply. Symmetric sidebands to the earth rotation-induced peak appear in the frequency range 50–76 Hz, and 76–99 Hz. These sidebands are due to the various mechanical resonances of the ring base which are excited by motion of the building. For an analysis, see Section III.

With a filter whose bandwidth (full width at half maximum) is 164 MHz to suppress sidelobes in the frequency domain, we observe the data in Table I for the three earth

TABLE I
EXAMPLE OF EVALUATION OF ONE RUN

	Earthline	Double Line	Triple Earthline
Center frequency (Hz)	76.1238 ± 0.0011	152.2474 ± 0.0020	228.3698 ± 0.0026
Base frequency (Hz)	76.1238 ± 0.0011	76.1237 ± 0.0010	76.1233 ± 0.0009
Linewidth (FWHM)			
With window (Hz)	0.1649 ± 0.0027	0.1740 ± 0.0048	0.1830 ± 0.0074
Without window (Hz)	0.0684 ± 0.0015	0.0831 ± 0.0040	0.1151 ± 0.010

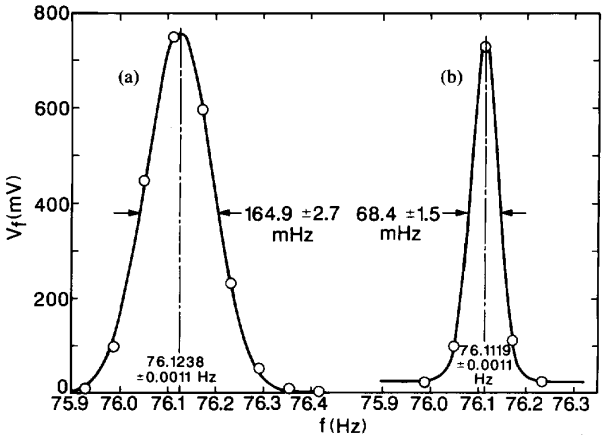

Fig. 3. Fit of Gaussians (continuous lines) to the measured Fourier components of the earthline (circles). 3(a) From a run that was prefiltered to avoid sidelobes. 3(b) Without prefiltering. The best-fitted parameters full-width-at-half-maximum (FWHM) and center-of-line are given, together with their errors.

lines (see also Fig. 3(a)). The equivalent base frequencies are the same within 1 MHz, while the errors given show that the evaluations are compatible.

Without filtering, the linewidths are much smaller, see Fig. 3(b). The harmonics are no longer dominated by the time window; the net ring laser linewidth is in this run thus determined by deconvolution as 32 ± 2 MHz in [10], together with further details of the statistical analysis of the prototype output.

The precision of the determination of line position, 1 MHz, is a fraction 2.3×10^{-18} of the laser frequency at 474 THz. As a fraction of the earth rotation peak (76 Hz in Fig. 2), the relative precision is 1 MHz/76 Hz = 1.3×10^{-5}.

Under simplified conditions we expect noncorrelated white noise in the beams. If observed through a square window in time (duration T), the rms frequency fluctuation of the beat frequency is expected to be

$$\Delta f_{\text{rms}} = [2hf_0^3/Q^2P_0T]^{1/2}. \quad (2)$$

With a measured decay time of $\tau = 15$ μs ($Q = 4.5 \times 10^{10}$), a measurement duration of $T = 16.384$ s, and an estimated power loss of $P_0 = 1$ μW (the latter is difficult to ascertain), we calculate $\Delta f_{\text{rms}} \sim 2$ MHz due to quantum noise. A few estimates of the sensitivity of the instrument for various planned experiments are given in Section IV.

III. CALIBRATION OF RING LASER OUTPUT

It is of considerable importance to know the properties of the ring laser as a transducer for measuring nonreciprocal effects. To this end, we report here an analysis of the satellite frequencies ("sidebands") b and d in Fig. 2, in particular those due to the prominent lines arising from the ring laser base resonance (which was also directly measured) at $f_T = 11.306 \pm 0.009$ Hz, with the relatively high quality factor $Q = 34$.

This ring laser base resonance was determined to generate a peak-to-peak angular motion of 1.1 μrad, which produced satellites whose relative amplitudes agree with standard frequency-modulation theory, four being above the noise. The latter also predicts that these sidelobes should have an equidistant frequency separation of f_T. Their center frequencies are plotted in Fig. 4 (filled circles) versus the order of the sidelobe, where zero corresponds to the earth line itself. A straight line in Fig. 4 verifies this; it has a slope of 11.300 ± 0.010 Hz. The agreement between the values of this slope and of f_T demonstrate the linearity of the ring laser as a transducer. The sidelobes cover the frequency range of 53 to 98 Hz.

A much larger frequency range is covered by the 50 Hz sidelobes, namely from 26 Hz to 226 Hz. The four analysed sidelobe frequencies are plotted in Fig. 4 as hollow dotted circles. The fitted straight line has a slope of 50.0162 Hz, compared to a measured 50 Hz line center of 50.0155 ± 0.0010 Hz. This fit is particularly good, the residuals in this case having an rms value of 6.3 mHz.

We would like to include a word of caution; while the table resonance satellites at 11.306 Hz stem clearly from a mechanical frequency modulation of the earth line and suffice to show the extreme linearity of the device, the 50 Hz satellites may not necessarily have the same cause; as already suggested above, the satellites could be partly due to the effects of hum at the international power line frequency of 50 Hz and its harmonics, giving rise to amplitude modulation of the optical beam through the RF excitation.

This result is exceedingly simple: Any additional oscillatory effect such as an oscillatory rotation will produce sidelines to the earth rotation line at a spacing given precisely by their oscillation frequency, even if (as in our case) the earth rotation line itself suffers systematic shifts (up to several hertz) from the value given by (1). The situation is equivalent to frequency modulation with a drifting carrier frequency (which in our case is the Sagnac

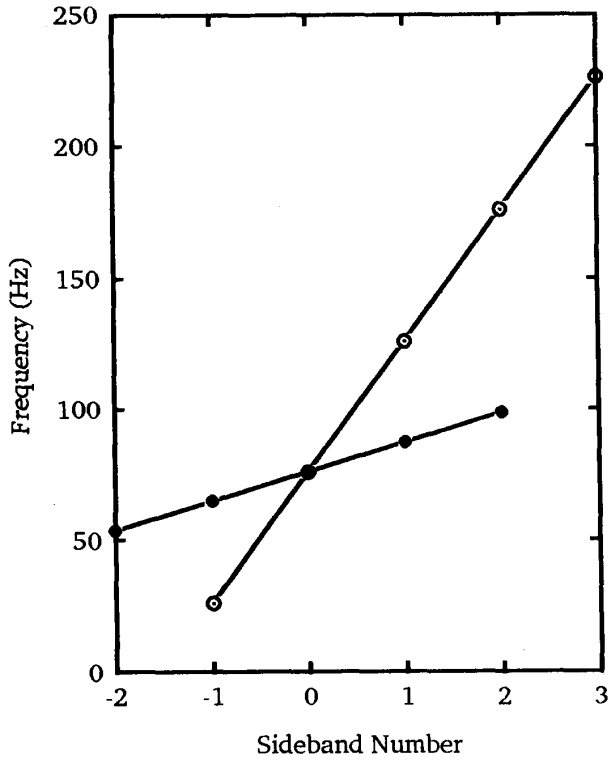

Fig. 4. Calibration of the spectrum. The frequency differences of the satellites to the earth line are plotted versus their order. The solid circles represent positions of the satellite frequencies to the earth line due to the 11.306 Hz mechanical resonance of the ring laser support; the open circles are from the 50 Hz vibrations. The vertical error bars are all less than 15 MHz rms and therefore are not visible. The slopes, in hertz, equal the two basic sideband frequencies.

frequency of the earth line). The relative positions of the modulation frequencies are not thereby affected.

IV. Future Applications of Ring Lasers

A. Seismography

The ring will sense rotation of the base on which it is mounted, or generally the curl of the absolute velocity. For example, if a horizontal shear wave from seismic activity moves the base, the ring output will show side bands to the earth's rotation, whose amplitudes are proportional to the linear amplitude of the seismic wave. Expressed as a limit of sensitivity to rotation, the results above give at present $(10^{-3}\ \text{Hz}/68\ \text{Hz}) \times (2\pi/\text{day}) \simeq 1 \times 10^{-9}\ \text{rad/s}$. From [11], we estimate a level of microseisms that is within the reach of such rings.

The sensitivity to additional rotation of the ring base is seen in Fig. 1 where sidebands to the earth line of up to about 50 Hz are created. We independently verified with motion detectors that the mounting base of the ring has torsional resonances in that range, with a quality factor of $Q = 34$. Such torsional resonances are excited by building vibrations: It was found impossible to get good spectra during business hours, or even at night under windy conditions; the ring was on the sixth floor of a nine-story building when the data presented in Figs. 1–4 were taken. At present, the ring is being transferred into a cave on Banks Peninsula near Christchurch, New Zealand, where it will be mounted on a concrete socket directly to the granite of an 11 million-year-old volcano. One of the uses is the detection of secondary shear waves, or any waves with a curl of ground velocity. The site is 131 km off the very active Indian–Pacific tectonic plate boundary and 5.8 km from the Pacific ocean. Thus we will be in a good position to evaluate the ring's potential as a seismographic detector of a novel kind.

It is complementary to methods like very-long-baseline interferometry [12], [13] which are sensitive to translation only. As opposed to classic seismographs the ring needs no external reference, nor a virtual reference, since it is an indicator of absolute rotation. Seismic activity will be observed as a time-dependent frequency (or phase) deviation from the average earth rate. For example, the seismometer installed at the present site of the ring laser shows as a predominant feature a background at 0.2 Hz, with 4 μm peak-to-peak displacement which originates from interaction of the air mass with oceans, and is observed at all coastal stations within several hundred kilometers from the coastline. As an early application we will attempt to measure the curl of this ground motion; it should appear as side lobes to the earth line at ± 0.2 Hz, etc.

B. Nonreciprocal Optical Pathlength Variations

A rough estimate of the minimum required nonreciprocal change along the beam path for an observable signal is $(n^+ - n^-) \simeq \Delta f/f \simeq 0.001/474 \times 10^{12} \sim 2 \times 10^{-18}$ which improves presently known measurement limits of such effects by several orders of magnitude [14].

Any phenomenon that influences the effective optical path of the ring in this way can be considered a candidate for a ring laser experiment. This includes searches for various conceivable nonlinear field-induced properties of vacuum and of material media, for example all types of Fresnel drag. In this latter case, the confirmation of the role of Lorentz and Laub drag by earlier precision experiments [8], [15] is still incomplete, since in these cases either the residual discrepancies in the experiment were greater than the statistical errors, or else the theoretical analysis was insufficiently refined compared to the capabilities of modern experiments such as the present ring. These and other applications are discussed in more detail in Stedman *et al.* [16], where the potential of this ring for a wide-ranging set of applications in fundamental physics is analysed and a first upper bound for a novel special-relativity-violating parameter is estimated.

V. Conclusion

The 0.75 m^2 area of our ring laser is sufficient for it to be unlocked by the Sagnac effect arising from the very stable earth rotation alone and with no other means of biassing. The lines in the Fourier transform of the ring interferometer output had a width of 32 Hz convolved

with the width due to the finite observation time of 16 s. The net width is approximately an order of magnitude above the estimated quantum noise limit. We observed pulling and pushing of the earth line of up to several hertz due to Adler pulling and susceptibility changes. We are currently seeking to include a frequency stabilization of one of the counterrotating beams with an external iodine cell to reduce the drift associated with susceptibility changes. Calibration of additional oscillatory phenomena is however both simple and precise, since they give rise to sidebands which are placed very precisely at the appropriate frequencies (see Section III). Harmonics of the earth rotation line which are produced by the nonlinearity of the laser gain medium were used to evaluate the frequency resolution of the line centers as being approximately 1 MHz. The accuracy with which the relative frequency of the sidebands may be determined is better than 10 MHz over a frequency range of 26–226 Hz. The extreme linearity will allow us to determine easily the lock-in threshold frequency, since the lines can be shifted by applying a transverse magnetic field to the plasma. A sensitivity of 10^4 Hz/T has been observed for such shifts.

Acknowledgment

The authors thank A. W. Louderback of Ojai Research, Ojai, CA, for his generous supply of our project with mirrors. The authors especially wish to thank B. G. Wybourne, the former Head of the Physics Department at the University of Canterbury for his unflagging support of the experiment, and F. V. Kowalski, School of Mines, Golden, CO, for substantial help during the construction phase of the ring.

References

[1] R. V. Pound and J. L. Snider, "Effect of gravity on gamma radiation," *Phys. Rev.*, vol. 140, pp. B788–B803, 1965.

[2] J. Vanier, "The active hydrogen maser: state of the art and forecast," *Metrologia 18*, pp. 173–186, 1982; Hellwig, H. W., *Proc. IEEE* 63, "Atomic frequency standards: a survey," pp. 212–229, 1975.

[3] E. J. Post, "Sagnac effect," *Rev. Mod. Phys.*, vol. 39, pp. 475–493, 1967.

[4] W. W. Chow, J. Gea-Banacloche, L. M. Pedrotti, V. E. Sanders, W. Schleich, and M. O. Scully, "The ring laser gyro," *Rev. Mod. Phys.*, vol. 57, pp. 61–104, 1985.

[5] H. Statz, T. A. Dorschner, M. Holtz, and I. W. Smith, *The Multioscillator Ring Laser Gyroscope*, M. L. Stitch and M. Bass, eds. pp. 229–332, Laser Handbook vol. 4, (North-Holland, 1985).

[6] T. A. Dorschner, H. A. Haus, M. Holtz, I. W. Smith, and H. Statz, "Laser gyro at quantum limit," *IEEE J. Quantum Electron.*, QE-16, pp. 1376–1379, 1980.

[7] M. R. Sayeh and H. R. Bilger, "Flicker noise in frequency fluctuations of lasers," *Phys. Rev. Lett.*, vol. 55, pp. 700–702, 1985.

[8] H. R. Bilger and W. K. Stowell, "Light drag in a ring laser: An improved determination of the drag coefficient," *Phys. Rev.*, vol. A16, pp. 313–319, 1977.

[9] G. E. Stedman, *Diagram Techniques in Group Theory*. Cambridge, UK: Cambridge University Press, 1990.

[10] G. E. Stedman and H. R. Bilger, "Ringlaser, an ultrahigh-resolution detector of optical nonreciprocities," *Digital Signal Processing*, vol. 2, pp. 105–109, 1992.

[11] A. Giazotto, "Interferometric detection of gravitational waves," *Phys. Rep.*, vol. 182, pp. 365–424, 1989.

[12] D. S. Robertson, "Geophysical applications of very-long-baseline interferometry," *Rev. Mod. Phys.*, vol. 63, pp. 899–918, 1991.

[13] U. Schreiber, Fundamentalstation Wettzell, Germany, private communication.

[14] E. Iacopini *et al.*, "On a sensitive ellipsometer to detect the vacuum polarization induced by a magnetic field," Nuovo Cimento, vol. 61B, pp. 21–37, 1981.

[15] G. A. Sanders and S. Ezekiel, "Measurement of Fresnel drag in moving media using a ring resonator technique," *J. Opt. Soc. Am.*, vol. B5, pp. 674–678, 1988.

[16] G. E. Stedman, H. R. Bilger, Li Ziyuan, M. P. Poulton, C. H. Rowe, I. Vetharaniam, and P. V. Wells, "Canterbury ring laser and tests for nonreciprocal phenomena," *Austral. J. Phys.*, vol. 46, pp. 87–102, 1993.